OPEN

miR-26b-5p suppresses chemoresistance in breast cancer by targeting serglycin

Qiwei Du[a,*], Zuguo Yuan[b,*], Xiaoling Huang[c,*], Yuqing Huang[a], Jie Zhang[d] and Rongguo Li[a]

Chemoresistance is a crucial barrier to limit the therapeutic outcome of breast cancer (BC), and the mechanism underlying chemoresistance development in BC is not fully understood. In this study, we aimed to investigate the potential involvement of miR-26b-5p/serglycin (SRGN) axis in BC drug resistance. The expression level of SRGN in drug-resistant BC cells was investigated by western blotting analysis, real-time quantitative PCR (qRT-PCR), immunohistochemical staining, and ELISA. Its expression between chemoresistant and sensitive patient samples was compared by qRT-PCR. Bioinformatics tool and dual-luciferase reporter assay were employed to identify miR-26b-5p as a regulator of SRGN. Functional assays were performed to examine cell proliferation, cell viability, apoptosis, migration, and invasion ability *in vitro*. Xenograft tumorigenesis experiment was conducted to evaluate the tumor suppressor effect of miR-26b-5p on chemoresistant BC cells. SRGN expression was significantly upregulated in both chemoresistant BC cell lines and chemoresistant patient samples. miR-26b-5p was identified as an upstream regulator of SRGN. Overexpression of miR-26b-5p downregulated SRGN expression, overcame chemoresistance, and suppressed cell proliferation, migration, and invasion in BC cells. Overexpression of miR-26b-5p also suppressed the tumorigenesis of chemoresistant BC cells *in vivo*. Mechanistically, the downregulation of SRGN by miR-26b-5p decreased the expression of breast cancer drug-resistant protein and multidrug-resistant protein 1 in chemoresistant BC cells. Our study identified miR-26b-5p as a tumor suppressor which targets SRGN to sensitize BC cells to chemotherapeutics. These results suggest that miR-26b-5p and SRGN may serve as potential biomarkers and targets for BC chemotherapy. *Anti-Cancer Drugs* 33: 308–319 Copyright © 2021 The Author(s). Published by Wolters Kluwer Health, Inc.

Anti-Cancer Drugs 2022, **33**:308–319

Keywords: breast cancer, breast cancer drug-resistant protein, chemoresistance, miR-26b-5p, multidrug-resistant protein 1, serglycin

[a]Department of Thyroid and Breast Surgery, The First People's Hospital of Xiaoshan, Hangzhou, [b]Chemoradiotherapy Center of Oncology, The Affiliated People's Hospital of Ningbo University, [c]Department of Obstetrics and Gynecology, Dongyang Women's and Children's Hospital, Dongyang and [d]Department of Breast Surgery, The First People's Hospital of Fuyang, Hangzhou, China

Correspondence to Rongguo Li, MD, Department of Thyroid and Breast Surgery, The First People's Hospital of Xiaoshan, No.199 Shixin South Road, Xiaoshan District, Hangzhou 311200, Zhejiang, China
Tel: +86 18158718317; e-mail: tiuk112@163.com

*Qiwei Du, Zuguo Yuan and Xiaoling Huang contributed equally to the writing of this article.

Received 19 June 2021 **Revised form accepted** 25 October 2021

Introduction

Breast cancer (BC), a common malignancy in women, has shown the tendency of an increasing incidence in recent years [1]. The International Agency for Research on Cancer reported that BC has officially replaced lung cancer as the most prevalent cancer in the world in 2020 [1]. Although a myriad of chemotherapy drugs can serve in the treatment of BC patients, the period of drug response is very short due to the rapid emergence of drug resistance [2]. Therefore, chemotherapeutic resistance is the key factor limiting therapeutic effects in BC, leading to a dismal clinical outcome for patients [2–4]. Previous studies on different cancers suggest that chemotherapy resistance is caused by genetic mutations and epigenetic alterations, which eventually promotes the features of tumor stem cells, increases the expression of drug efflux proteins, and enhances the antiapoptotic signaling pathways [5,6]. However, the mechanisms underlying drug resistance in BC remain confounding. Understanding the molecular targets or biomarkers for BC chemoresistance will provide insights into drug selection and prioritization for a more effective BC treatment.

Long noncoding RNAs (LncRNAs), a class of cellular RNAs with a length of over 200 nucleotides, play vital roles in tumor biology such as tumor initiation, progression, and drug sensitivity [7]. LncRNAs can regulate gene expression by interfering with posttranscriptional processes [8]. Some lncRNAs are also involved in transcriptional regulations by interacting with chromatin-modifying complexes or DNA regulatory elements [8,9]. Because dysregulation of multiple lncRNAs has been identified in BC [7], functional characterization of

these molecules and their downstream targets could provide opportunities for therapeutic intervention.

Serglycin (SRGN) is a glycoprotein that is exported to the extracellular matrix, and it is shown to be involved in the storage and secretion of intracellular substances [10]. SRGN has been proposed as a drug resistance indicator in various cancers, including colorectal cancer, ovarian cancer, and non-small cell lung cancer [10–12]. A recent study revealed that SRGN activates the ITGA5/FAK/CREB/YAP signaling pathway and promotes HDAC2 expression to maintain chemoresistance and stemness of BC cells [13]. However, the regulatory mechanism governing SRGN expression remains elusive in BC cells. In this study, we investigated the molecular mechanisms underlying the regulation of SRGN expression and discovered that SRGN expression could be inhibited by miR-26b-5p. miR-26b-5p seemed to be downregulated in chemoresistant BC tissues and cells to maintain a high level of SRGN. Accordingly, SRGN could upregulate the expression of BC resistance proteins such as breast cancer drug-resistant protein (BCRP) and multidrug-resistant protein 1 (MRP1). Together, our data suggest that miR-26b-5p/SRGN could serve as a potential target for overcoming chemoresistance in BC cells.

Materials and methods

Cell culture and transfection

MCF-7, MDA-MB-231, and MB453 cells [American Type Culture Collection (ATCC)] were cultured in RPMI-1640 medium (Gibco, Carlsbad, California, USA) containing 10% fetal bovine serum (Gibco), according to ATCC's instructions. Chemoresistant cell lines MCF-7/DOX and MDA-MB-231/DPP were established by a continuous culturing of MCF-7 and MDA-MB-231 cell lines with increasing dosage (0.1-100 μg/ml) of doxorubicin (DOX, Cat# HY-15142; MedChemExpress, Monmouth Junction, New Jersey, USA) or cisplatin (DPP, Cat# HY-15142, Cat# HY-17394; MedChemExpress) for 6 months. The medium was changed every 4 days.

The transection of small interfering RNA (siRNA), plasmid, mRNA mimic, or inhibitor was performed using Lipofectamine 3000 reagent (Thermo Fisher Scientific, Waltham, Massachusetts, USA). Briefly, in a six-well plate, 60% confluent cells were transfected with 100 nM of mRNA mimic, inhibitor, siRNA, or 6 μg of pcDNA3.1-SRGN expression plasmid according to manufacturer's instruction. Transfected cells were subjected to subsequent analysis 48 h post-transfection. siRNA targeting SRGN (siSRGN) and negative control (si-NC) were synthesized by GenePharma (Shanghai, China). miR-26b-5p inhibitor, mimic, and negative controls (mim-NC and miR-NC) were synthesized by Keygen Biotech (Nanjing, China).

Patients

This study was approved by the ethical review committee of the First People's Hospital of Xiaoshan and all enrolled patients signed the informed consent. Tissue samples were collected from 60 BC patients by surgery after chemotherapy in The First People's Hospital of Xiaoshan from 2018 to 2020. The 60 patients were divided into chemoresistant patients (n = 20) and chemosensitive patients (n = 40).

RNA extraction and real-time quantitative PCR

Trizol reagent (15596026; Thermo Fisher Scientific) was used to extract RNA from tissues and cells according to the instructions. The extracted total RNA was dissolved in diethylpyrocarbonate water and its concentration was measured with NanoDrop. A total of 1 μg of total RNA was used for reverse transcription using PrimeScript RT Master Mix (Takara, Shanghai, China). The resulting cDNA was analyzed in a 7500 Real-Time PCR System (Applied Biosystems/Life Technologies, Carlsbad, California, USA) using SYBR premix EX Taq II kit (RR820A; Takara, Dalian, China). The PCR cycling condition used was as follows: 95°C for 2 min, 40 cycles of 95°C for 30 s, 60°C for 30 s, and 72°C for 60 s. The · method was used to analyze the relative expression level and GAPDH was used as the internal reference gene. All primer sequences were synthesized and purchased from Shanghai Sangon Biotechnology Co., Ltd. (Shanghai, China) and are presented as follows:

miR-26b-5p: F, 5′-CCTGTGGAGATTGATGGGGT-3′ and R, 5′-TCTCTGGGCCTCTGACATTC-3′; SRGN: F, 5′-GCAAGTGTCCTTAAGTCAA-3′ and R, 5′-CGAAAGTGATGCTTTCCAT-3′; GAPDH: F, 5′-CCACTGGCATCGTGATGGA-3′ and R, 5′-CGCT CGGTGAGGATCTTCAT-3′.

Western blotting analysis and ELISA

Total protein was extracted from cells or tissues using radioimmunoprecipitation analysis (RIPA) lysis buffer containing protease inhibitor cocktail (78429; Thermo Fisher Scientific). Samples suspended in RIPA buffer were lysed on ice for 10 min and then centrifuged at 14 000 rpm for 10 min. The supernatant containing total protein lysate was quantified by a BCA Protein Assay Kit (P0009; Beyotime Biotechnology, Shanghai, China). A total of 10 μg protein was used for SDS-PAGE electrophoresis. The separated protein in SDS-PAGE gel was transferred onto the polyvinylidene difluoride membrane. After blocking with 5% skimmed milk for 1 h, the membrane was then incubated with primary antibodies: anti-SRGN (1:1000, PA5-113691; Thermo Fisher Scientific), anti-BCRP (1:1000, #42078; Cell Signaling Technology), and GAPDH (1:2000, #2118; Cell Signaling Technology) overnight at 4°C. The membrane was washed three times with Tris-buffered saline with Tween-20 (TBST) and further incubated with horseradish peroxidase (HRP)-linked secondary antibody (1:3000, #7074; Cell Signaling, Massachusetts, USA) at room temperature for 1 h. Then, the membrane was washed four times with TBST and the protein bands were visualized using an enhanced chemiluminescence kit (Santa Cruz, Texas, USA, sc-2048) and photographed

on a gel imager system (Bio-Rad, Hercules, California, United States). The densitometry analysis was performed with ImageJ software (National Institutes of Health, Bethesda, Maryland, USA).

ELISA

Cell culture supernatants were collected and analyzed with ELISA Kit for serglycin (Cat# SEC869Hu; Cloud-Clone Corp., Katy, Texas, USA), according to the instructions. Briefly, 100 µl cell culture supernatant from 80% confluent cells in a six-well plate was added to the 96-well assay plate for 1-h incubation at 37°C. A serial dilution of the standards in the kit was assayed at the same time to generate the standard curve. The samples were aspirated and 100 µl Detection Reagent A was added to each well for 1-h incubation at 37°C. The solution was aspirated and each well was washed three times using the wash buffer. Then, 100 µl Detection Reagent B was added to each well for a 30-min incubation at 37°C. The solution was aspirated and each well was washed five times using the wash buffer. Next, 90 µl Substrate Solution was added to each well and the plate was incubated for 15 min at 37°C. Finally, 50 µl Stop Solution was added and the absorbance in each sample was measured at 450 nm immediately on a microplate reader (Infinite M200 PRO, Tecan, Barcelona, Spain).

Viable cell count, cell viability, and colony formation assay

Cells were digested by trypsin and resuspended in PBS containing 0.4% trypan blue solution at the ratio of 9:1. After staining for 3 min, the live cells and dead cells (stained blue) were counted, and the cell viability was calculated as the proportion of live cells in the total number of cells.

Cell Counting Kit-8 (CCK-8, Cat# K1018; APExBIO, Houston, Texas, USA) was used for cell proliferation assay. Cells were seeded into a 96-well plate at a density of 1500 cells/well and cultured in a humidified cell culture incubator for 0, 24, 48, 72, and 96 h, respectively. Subsequently, 10 µl CCK-8 reaction solution was added to the cell culture at the indicated time point and incubated for 1 h in a humidified cell culture incubator. The light absorption value (OD value) in each condition was captured at 450 nm wavelength on a Synergy H1 microplate reader (Winooski, Vermont, USA).

For colony formation assay, cells were trypsinized and seeded into a six-well plate (1000 cells/well) and cultured for 14 days. The culture medium was changed every 3 days during the period. After 14 days, cells were fixed with 4% paraformaldehyde at room temperature for 10 min and stained with 0.5% crystal violet (Beyotime, Shanghai, China) for 20 min. Subsequently, the number of colonies was counted and the morphology of the colonies was photographed under Leica AM6000 microscope (Leica, Wetzlar, Germany). Five regions were randomly selected under the microscope and the number of colonies was counted. A collection of more than 50 cells was considered as a cell colony.

Transwell migration and invasion assays

Cells with different treatments were trypsinized and resuspended in a serum-free medium. The transwell upper chamber (#3401; Corning, New York, USA) without Matrigel (#356234; BD Biosciences, Bedford, Massachusetts, USA) was used for migration assay, whereas transwell upper chamber coated with Matrigel was used for invasion assay. A total of 1×10^6 cells were inoculated into the transwell upper chamber in a serum-free medium and 500 µl of 10% serum-containing medium was added to the lower chamber. After 18 h, the culture medium was discarded and the cells were fixed with 4% paraformaldehyde at room temperature for 10 min and stained with 0.5% crystal violet (Beyotime) for 20 min. Cells were photographed under Leica AM6000 microscope.

Flow cytometer apoptosis assay

The detection of cell apoptosis was performed using the FITC Annexin V Apoptosis Detection Kit (BD Biosciences, California, USA) according to manufacturer's instructions. Cells with different treatments were trypsinized and washed twice with 1× PBS, and resuspended in the staining solution. In brief, 1 µl Annexin V-FITC and 1 µl propidium iodide (PI) were added to the 1000 µl cell resuspension of one million cells and incubated for 15 min in the dark. Stained cells were centrifuged and washed twice with 1× PBS and resuspended in 400 µl PBS. The percentage of apoptotic cells was detected by BD FACS CantoTM II Flow Cytometer (BD Biosciences).

Immunohistochemistry

Tissue samples from patients or animal models were fixed with 4% formaldehyde overnight and then embedded in paraffin. Tissues were cut into 10-µm sections before staining. The tissue section was deparaffinized and hydrated, and the antigen unmasking was performed by heating the section in 1× citrate unmasking solution [SignalStain Citrate Unmasking Solution (10×), #14746; Cell Signaling Technology] at 95°C for 10 min. Sections were cooled for 30 min and washed three times in TBST buffer. After blocking for 1 h in TBST with 5% normal goat serum, the section was incubated with primary antibody anti-Ki67 antibody (1:500 dilution, #S9129; Cell Signaling Technology) and anti-SRGN antibody (1:500 dilution, #sc-374657; Santa Cruz) overnight at 4°C. The section was washed three times using TBST buffer and then soaked with 1–3 drops of SignalStain Boost Detection Reagent (HRP, Rabbit #8114; Cell Signaling Technology) for 30 min at room temperature. Then, 200 µl SignalStain substrate (#8059; Cell Signaling Technology) was added to each section for 5 min. The section was washed in distilled water twice for 5 min each and then dehydrated. The section was then mounted with coverslips using a mounting medium (#14177; Cell Signaling Technology) before imaging.

Fig. 1

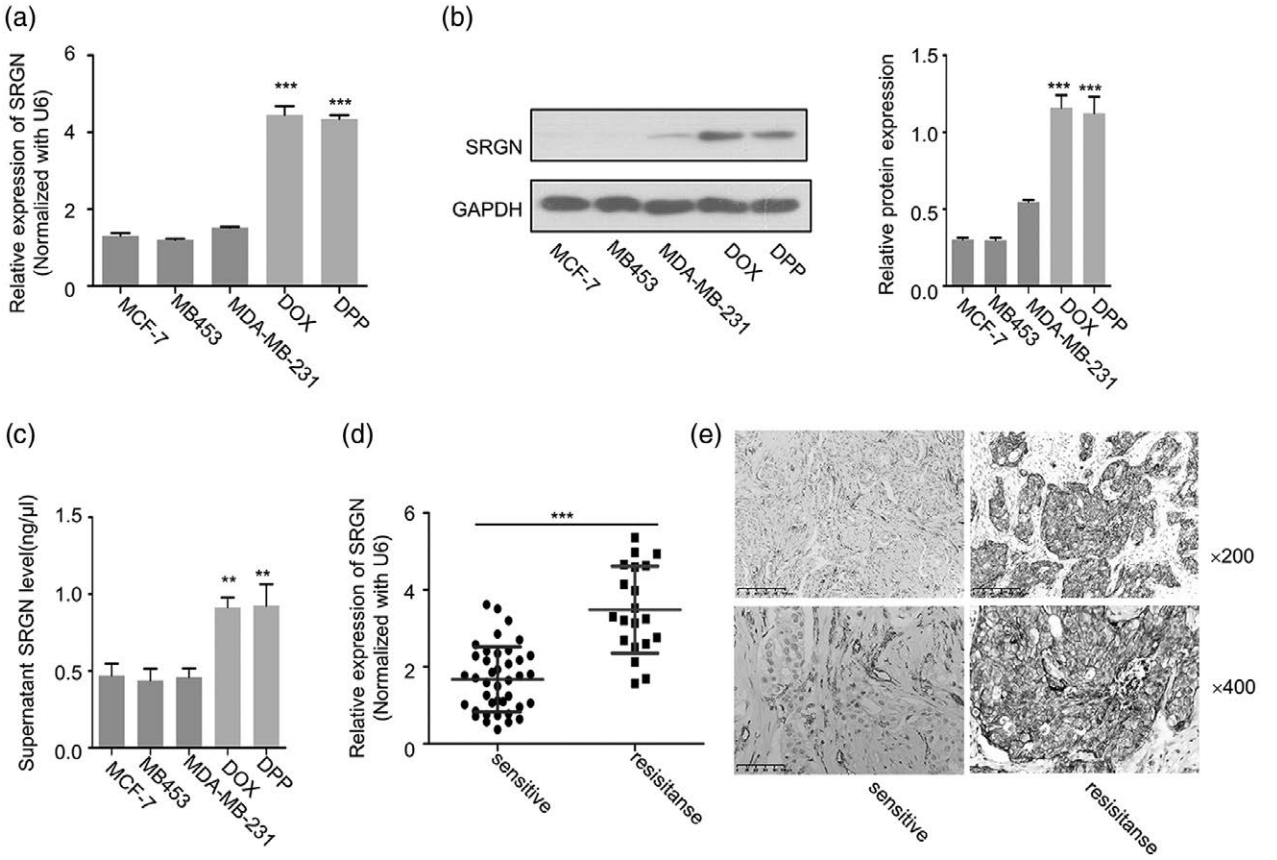

SRGN expression is significantly upregulated in chemoresistance BC cell lines. (a) SRGN expression in parental cell lines (MCF-7, MDA-MB-231, and MB453) and drug-resistant cell lines (MCF-7/DOX and MDA-MB-231/DPP) was measured by qRT-PCR; ***$P < 0.001$. (b) SRGN protein levels in the indicated BC cell lines were detected by western blot analysis; ***$P < 0.001$. (c) ELISA measurement of SRGN protein levels in cell culture medium of parental and drug-resistant cell lines; **$P < 0.01$. (d) SRGN mRNA levels in tissues of BC patients (chemotherapy sensitive or resistant) were measured by qRT-PCR; ***$P < 0.001$. (e) Immunohistochemistry staining of SRGN expression in chemotherapy-sensitive or -resistant BC tissues. BC, breast cancer; DOX, doxorubicin; DPP, cisplatin; qRT-PCR, real-time quantitative PCR; SRGN, serglycin.

Luciferase reporter assay

To demonstrate the functional interaction between miR-26b-5p and SRGN mRNA, the sequence containing the wild-type (WT) binding site and the sequence with the mutated binding site in the 3′-untranslated region (UTR) of SRGN mRNA was cloned into the PmirGLO reporter vector (Promega). The reporter plasmid and *Renilla* luciferase (hRlucneo) control plasmid were cotransfected into cells with either miR-26b-5p mimic or miR-NC using Lipofectamine 3000 reagent according to manufacturer's instructions (Invitrogen). Forty-eight hours post transfection, the relative luciferase activities were measured using Dual-Luciferase Reporter Assay Kit (E1910; Promega) on a luminescence microplate reader (Infinite 200 PRO). The relative firefly luciferase activity in the reporter plasmid was normalized to that of *Renilla* luciferase (hRlucneo) in the control plasmid.

Xenograft tumorigenesis model

All animal procedures were approved by the animal care and use ethical committee of First People's Hospital of Xiaoshan. Twelve male immunodeficient nude mice (30-40 g) were randomly divided into two groups (six mice in each group): (1) mim-NC group (injected with MCF-7/DOX and transfected with miR-NC), (2) miR-26b-5p group (injected with MCF-7/DOX cells and transfected with miR-26b-5p). Next, 0.2 ml of cell suspension containing 1×10^7 cells was injected into the flank of each mice. Mice were injected intravenously with 10 mg/kg DOX every 7 days starting from the day of tumor cell inoculation. Tumor volumes were monitored at 7, 14, 21, 28, or 35 days post-injection. Tumor size was monitored using a caliper and the tumor volume was calculated using the formula: $V(\text{tumor}) = 0.5 \times \text{length} \times \text{width}^2$. Five weeks after tumor cell inoculation, all the mice were euthanized by CO_2 asphyxiation followed by subsequent

cervical dislocation. The tumors of terminally dead mice were resected for weight measurement and immunohistochemistry staining.

Statistical analysis

GraphPad Prism software (San Diego, California, USA) was used for the analysis of statistical significance. All experiments were repeated three times. The statistical difference between the two groups was compared using unpaired Student's *t*-test. Comparisons among multiple groups were performed by one-way analysis of variance (ANOVA) with Tukey's post hoc test for pairwise comparison. Comparisons of data at multiple time points were examined using two-way ANOVA. Spearman correlation analysis was performed to determine the correlation between gene expressions. Data were reported as the mean ± SD. $P < 0.05$ was considered to be statistically different.

Results

Serglycin upregulation is correlated with chemoresistance in breast cancer

To investigate the potential role of SRGN in drug resistance in BC cells, we first compared the mRNA and protein levels of SRGN between parental BC cell lines (MCF-7, MB453, and MDA-MB-231) and drug-resistant BC cell lines (MCF-7/DOX and MDA-MB-231/DPP). Real-time quantitative PCR (qRT-PCR) and western blot results showed that SRGN expression in drug-resistant BC cells was significantly higher than that of the parental cell lines (Fig. 1a and b). We also measured the secreted protein level of SRGN in the culture medium of BC cells by ELISA and found that there was a significant increase of SRGN protein in the culture medium of drug-resistant cell lines (Fig. 1c). To further validate the increased expression of SRGN in the clinical setting, we examined SRGN expression levels in tissues from 40 chemotherapy-sensitive and 20 chemotherapy-insensitive BC patients using qRT-PCR and immunohistochemical staining. Consistently, SRGN expression was significantly higher in the chemotherapy-resistant tissues as compared to chemotherapy-sensitive tissues (Fig. 1d and e). To further analyze the expression of SRGN and its clinical significance, the patients were divided into high SRGN expression (n = 30) and low SRGN expression (n = 30) groups based on the median expression level of SRGN. Chi-square test was used to assess the association of clinicopathological data of these patients with SRGN expression levels. Interestingly, high SRGN expression was associated with larger tumor size, more advanced tumor node metastasis (TNM) stages, lymph node metastasis, and the development of chemoresistance (Table 1). Collectively, these data suggest that the upregulation of SRGN may contribute to the development of drug resistance in BC cells.

Table 1 Correlations of serglycin expression level with clinicopathologic features of breast cancer patients

Patients	High SRGN ($n = 30$)	Low SRGN ($n = 30$)	*P* value
Age (years)			0.78989
≥51	19	18	
<51	11	12	
Tumor size			0.0034**
≤2 cm	7	16	
>2 cm	23	14	
Chemoresistance			0.00013**
No	13	27	
Yes	17	3	
Lymph node metastasis			0.01485*
No	6	15	
Yes	24	15	
TNM stage			0.00497**
I	2	8	
II	6	10	
III	7	9	
IV	15	3	
ER status			0.05206*
Positive	6	13	
Negative	24	17	
PR status			0.11805
Positive	10	18	
Negative	20	12	
HER-2 status			0.79576
Positive	15	14	
Negative	15	16	

The relationship between SRGN expression and BC clinicopathological data was analyzed by chi-square test.
BC, breast cancer; ER, estrogen receptor; PR, progesterone receptor; SRGN, serglycin; TNM, tumor node metastasis.
*$P < 0.05$.
**$P < 0.01$.

miR-26b-5p interacts with 3′-untranslated region of serglycin mRNA

To find the potential regulatory molecules in SRGN expression, we searched for the potential miRNAs targeting SRGN using the miRTarbase/miRWalk database. Our results showed that there was a predicted binding site of miR-26b-5p in the 3′-UTR region of SRGN mRNA (Fig. 2a). qRT-PCR analysis revealed that miR-26b-5p expression was significantly lower in drug-resistant BC cells (Fig. 2b). To confirm the functional interaction, we cloned the WT and mutated binding site of the 3′-UTR region of SRGN mRNA into a luciferase reporter to perform dual-luciferase reporter assay. The cotransfection of miR-26b-5p mimic significantly suppressed the luciferase activity in the WT reporter, whereas no inhibition was observed in the mutated reporter (Fig. 2c). Together, these data indicate that miR-26b-5p targets SRGN mRNA.

miR-26b-5p modulates serglycin expression in breast cancer cell lines

To further study whether miR-26b-5p could regulate the expression level of SRGN, we applied synthetic miR-26b-5p mimic and inhibitor in drug-resistant cell lines. The transfection of miR-26b-5p mimic or inhibitor in MCF-7/DOX and MDA-MB-231/DPP cells upregulated or downregulated the level of miR-26b-5p respectively (Fig. 3a). Importantly, miR-26b-5p mimic significantly suppressed SRGN expression at both mRNA and protein

Fig. 2

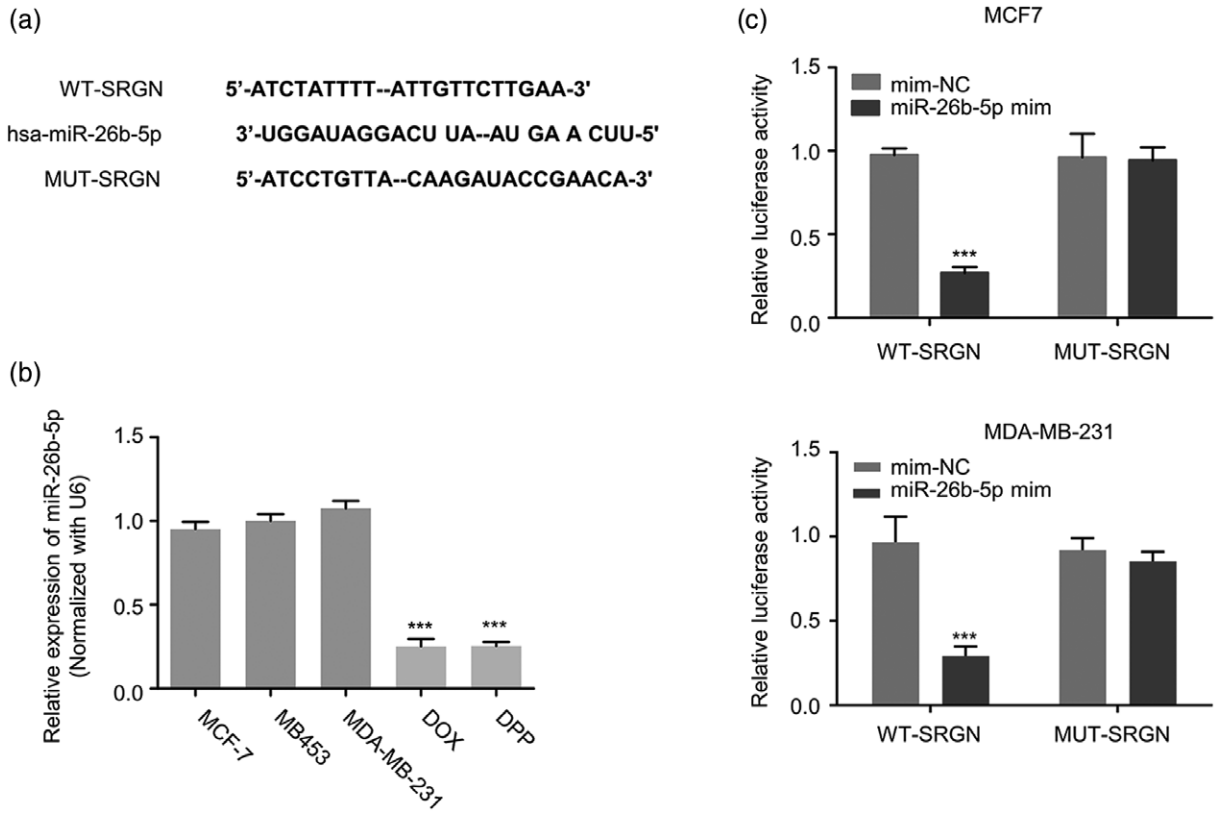

miR-26b-5p interacts with 3′-UTR of SRGN mRNA. (a) The binding site between miR-26b-5p and SRGN mRNA 3′-UTR was predicted by bioinformatics tools. (b) miR-26b-5p expression levels in BC cell lines were detected by qRT-PCR; ***$P < 0.001$. (c) Dual-luciferase reporter assay was performed in MCF-7 and MDA-NB-231 cell lines using WT or MUT reporter; ***$P < 0.001$. BC, breast cancer; MUT, mutant; qRT-PCR, real-time quantitative PCR; SRGN, serglycin; UTR, untranslated region; WT, wild type.

level, whereas miR-26b-5p inhibitor increased SRGN expression in both MCF-7/DOX and MDA-MB-231/DPP cells (Fig. 3b and c). In the patient samples, chemosensitive samples showed a significantly higher level of miR-26b-5p expression as compared to the chemoresistant ones (Fig. 3d). Furthermore, Spearman correlation coefficient analysis showed that there was a significant negative correlation between the expression levels of SRGN and miR-26b-5p in BC tumor samples (Fig. 3e). These data strongly indicate that miR-26b-5p negatively regulates SRGN expression in BC cells.

miR-26-5p mimic resensitizes breast cancer cells to chemotherapeutics and suppresses cell proliferation, migration, and invasion

We next examined cell viability by trypan blue staining assay in the presence of DOX and DPP, the chemotherapeutic drugs used to generate the drug-resistant cell lines [14]. miR-26b-5p mimic remarkably resensitized MCF-7/DOX and MDA-MB-231/DPP cells to the chemotherapeutic treatment, whereas inhibiting miR-26b-5p activity by miR-26b-5p inhibitor rendered the cells more resistant (Fig. 4a). Consistently, Annexin V and PI staining assay demonstrated that miR-26b-5p overexpression promoted apoptosis of drug-resistant cells, whereas miR-26b-5p inhibitor reduced the percentage of apoptotic cells after chemotherapeutic drug treatment (Fig. 4b). miR-26b-5p overexpression also attenuated cell proliferation and the colony formation ability of drug-resistant cells, whereas miR-26b-5p inhibitor enhanced cell proliferation and colony formation (Fig. 4c and d). In addition, cell migration and invasion abilities were also negatively regulated by miR-26b-5p (Fig. 4e and f). Together, our data suggest that miR-26-5p expression level could regulate drug sensitivity and the malignant phenotype in BC cells.

miR-26b-5p/serglycin axis regulates the expression of breast cancer drug-resistant protein and multidrug-resistant protein 1 in drug-resistant breast cancer cells

Previous studies have shown that BCRP and MRP1 are the main factors contributing to multidrug resistance (MDR) in BC [15–18]. We, therefore, investigated whether miR-26b-5p/SRGN axis regulates the expression of BCRP and MDR1 in MCF-7/DOX

Fig. 3

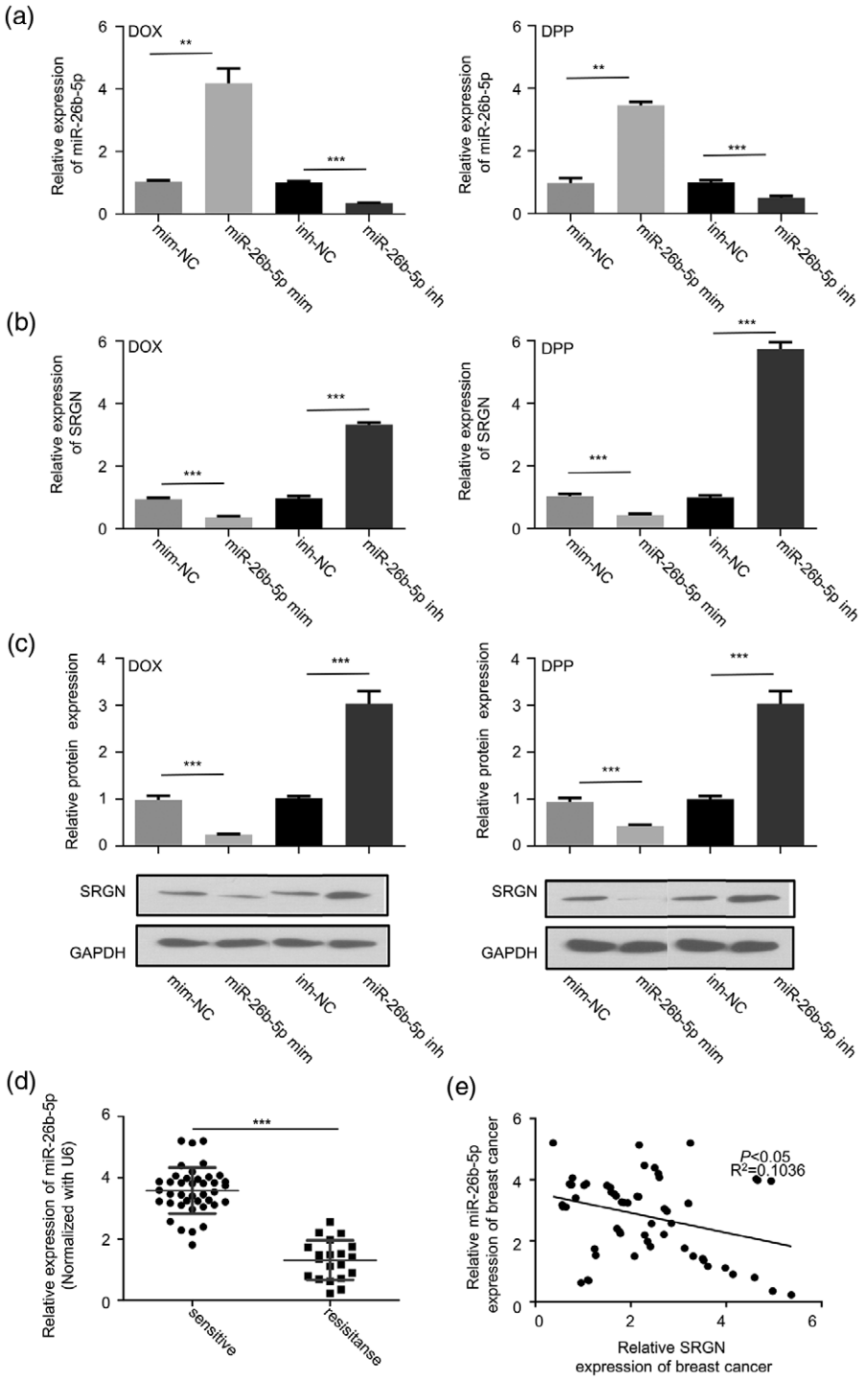

miR-26b-5p modulates SRGN expression in BC cell lines. (a) miR-26b-5p mimic and miR-26b-5p inhibitor were transfected into drug-resistant BC cells (MCF-7/DOX and MDA-MB-231/DPP). miR-26b-5p expression level after transfection was determined by qRT-PCR; $^{**}P < 0.01$, $^{***}P < 0.001$. (b) MCF-7/DOX and MDA-MB-231/DPP cells were transfected with miR-26b-5p mimic or miR-26b-5p inhibitor, and SRGN mRNA levels were measured by qRT-PCR; $^{***}P < 0.001$. (c) SRGN protein levels were detected by western blot analysis after miR-26b-5p mimic or miR-26b-5p inhibitor transfection; $^{***}P < 0.001$. (d) miR-26b-5p levels in BC tumor tissues were measured by qRT-PCR; $^{***}P < 0.001$. (e) Spearman correlation analysis between the expression levels of SRGN and miR-26b-5p in 60 BC tissues; $P < 0.05$. BC, breast cancer; DOX, doxorubicin; DPP, cisplatin; qRT-PCR, real-time quantitative PCR; SRGN, serglycin.

Fig. 4

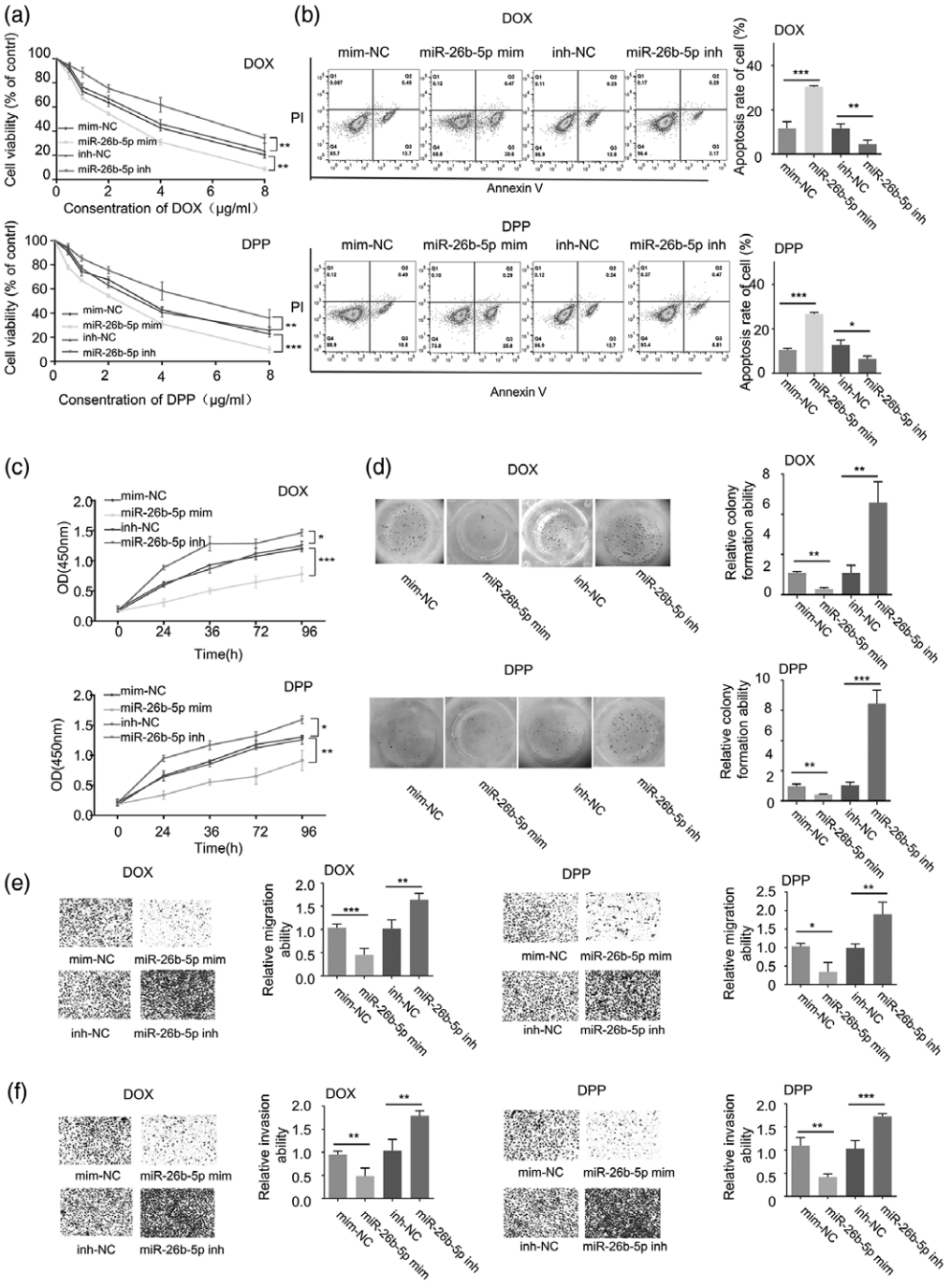

miR-26-5p mimic resensitizes BC cells to chemotherapeutics and suppresses cell proliferation, migration, and invasion. (a) Cell viability analysis (trypan blue assay) of MCF-7/DOX and MDA-MB-231/DPP cells transfected with miR-26b-5p mimic or inhibitor upon the treatment of different concentrations of DOX or DPP for 48 h; $^{**}P < 0.01$, $^{***}P < 0.001$. (b) MCF-7/DOX and MDA-MB-231/DPP cells transfected with miR-26b-5p mimic or inhibitor were treated with 2.0 μg/ml DOX or DPP for 48 h. Apoptosis was analyzed by Annexin V and PI staining via flow cytometry; $^{*}P < 0.05$, $^{**}P < 0.01$, $^{***}P < 0.001$. (c) Cell proliferation analysis with 2.0 μg/ml drug treatment in MCF-7/DOX and MDA-MB-231/DPP cells transfected with miR-26b-5p mimic or miR-26b-5p inhibitor by CCK-8 assay; $^{*}P < 0.05$, $^{**}P < 0.01$, $^{***}P < 0.001$. (d) Colony formation assay of MCF-7/DOX and MDA-MB-231/DPP cells transfected with miR-26b-5p mimic or miR-26b-5p inhibitor in the presence of 2.0 μg/ml drug; $^{**}P < 0.01$, $^{***}P < 0.001$. (e and f) Migration (e) and invasion (f) ability of MCF-7/DOX and MDA-MB-231/DPP cells transfected with miR-26b-5p mimic or miR-26b-5p inhibitor; $^{*}P < 0.05$, $^{**}P < 0.01$, $^{***}P < 0.001$. BC, breast cancer; CCK-8, Cell Counting Kit-8; DOX, doxorubicin; DPP, cisplatin; PI, propidium iodide; SRGN, serglycin.

Fig. 5

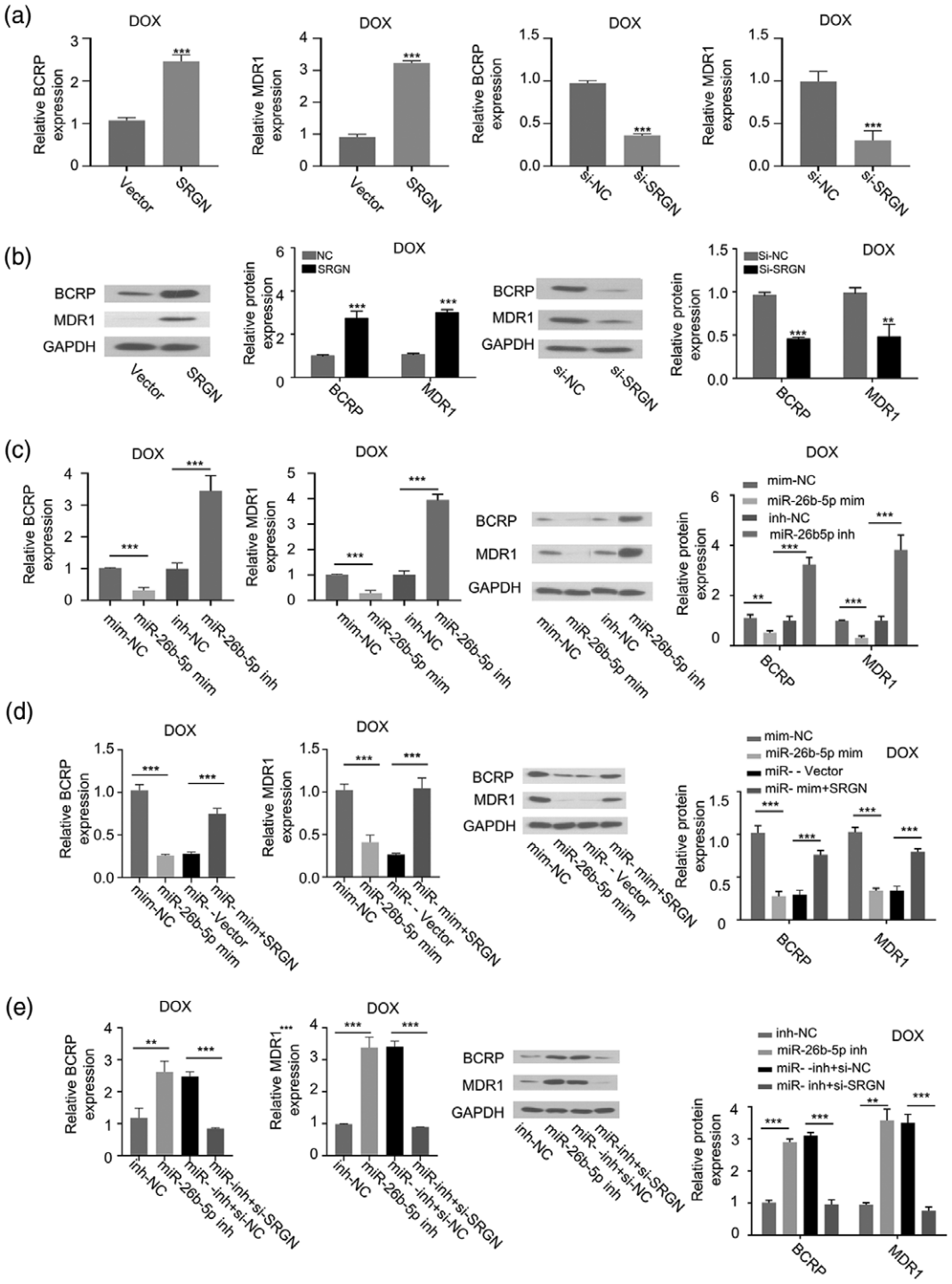

miR-26b-5p/SRGN axis regulates the levels of BCRP and MDR1 in chemoresistant BC cells. (a) qRT-PCR showing the mRNA levels and (b) western blot analysis showing the protein levels of BCRP and MDR1 in MCF-7/DOX cell lines overexpressing SRGN or with SRGN knockdown; $^{**}P < 0.01$, $^{***}P < 0.001$. (c) qRT-PCR and western blot analysis showing the mRNA and protein levels of BCRP and MDR1 in MCF-7/DOX cells transfected with miR-26b-5p mimic or inhibitor; $^{**}P < 0.01$, $^{***}P < 0.001$. (d) mRNA and protein levels of BCRP and MDR1 in cells with miR-26b-5p mimic and SRGN overexpression; $^{**}P < 0.01$, $^{***}P < 0.001$. (e) mRNA and protein levels of BCRP and MDR1 in cells with miR-26b-5p inhibitor and SRGN knockdown; $^{**}P < 0.01$, $^{***}P < 0.001$. BC, breast cancer; BCRP, breast cancer drug-resistant protein; DOX, doxorubicin; MDR1, multidrug-resistant protein 1; qRT-PCR, real-time quantitative PCR; SRGN, serglycin.

Fig. 6

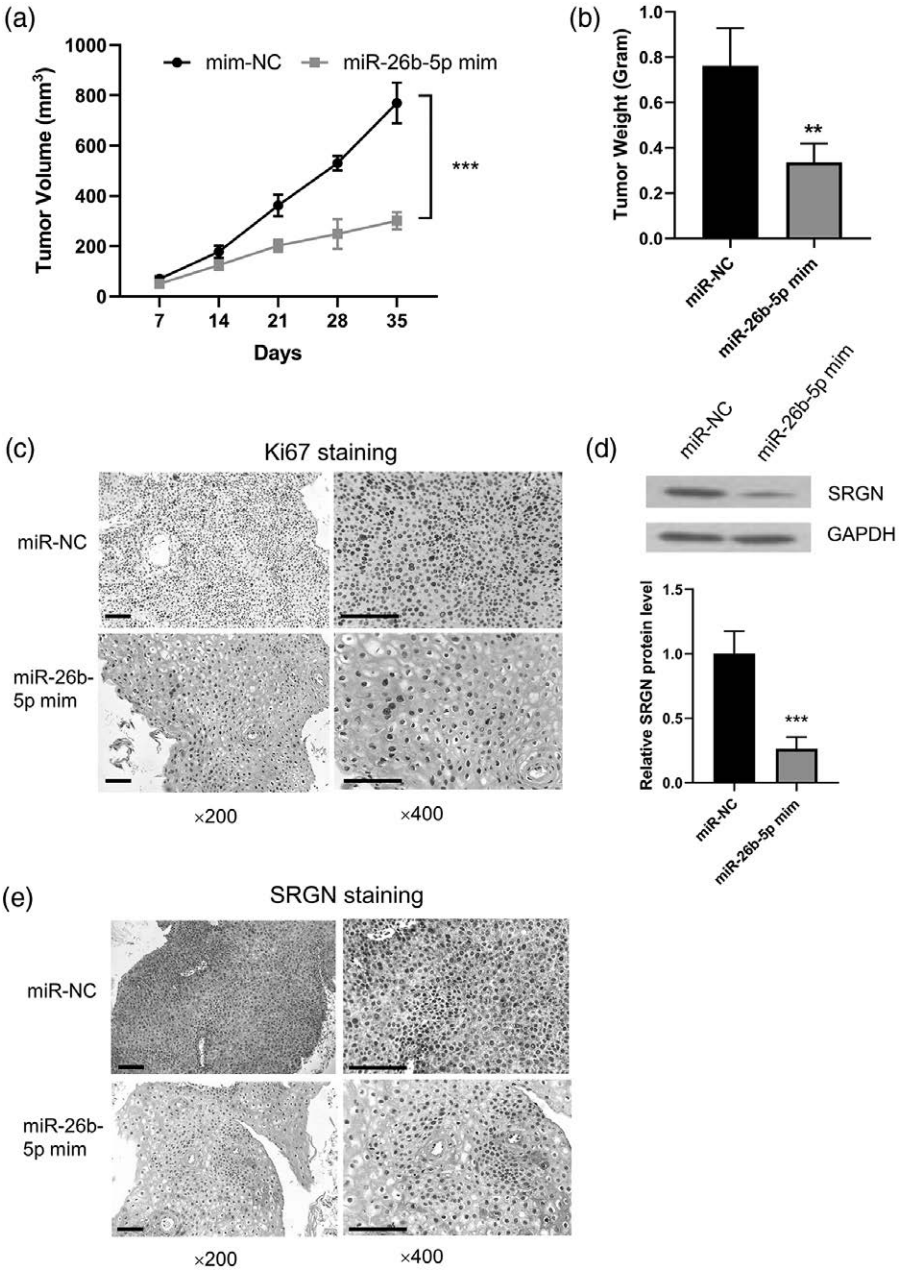

miR-26b-5p regulates drug response in a xenograft mouse model. (a) Twelve male immunodeficient nude mice (30-40 g) were randomly assigned to mim-NC group (injected with MCF-7/DOX and transfected with mim-NC; $n = 6$) and miR-26b-5p mimic group (injected with MCF-7/DOX cells and transfected with miR-26b-5p mimic; $n = 6$). Then, 0.2 ml of cell suspension containing 1×10^7 cells was injected into the flank of each mice. Mice were injected intravenously with 10 mg/kg DOX every 7 days. Tumor volume was monitored every week; $^{***}P < 0.001$. (b) Xenograft tumor weight in mim-NC and miR-26b-5p mimic group at the end of the experiment; $^{**}P < 0.01$. (c) IHC staining of Ki67 in tumor samples of mim-NC and miR-26b-5p mimic group. (d) Western blot analysis of SRGN protein level in tumor samples of mim-NC and miR-26b-5p mimic group; $^{***}P < 0.001$. (e) IHC staining of SRGN in tumor samples of mim-NC and miR-26b-5p mimic group. DOX, doxorubicin; IHC, immunohistochemistry; SRGN, serglycin.

cells. We transfected cells with SRGN expression vector or siRNA targeting SRGN (si-SRGN) and the corresponding controls. qRT-PCR and western blot analysis showed that SRGN overexpression upregulated the expression of BCRP and MDR1, whereas SRGN silencing downregulated their expression (Fig. 5a and b). Meanwhile, the expression of BCRP and MDR1 was significantly reduced after the transfection with miR-26b-5p mimic and increased after miR-26b-5p inhibitor transfection in MCF-7/DOX cells (Fig. 5c). Importantly,

SRGN overexpression could rescue the level of BCRP and MDP1 after miR-26b-5p mimic treatment (Fig. 5d). In contrast, cotransfection of SRGN siRNA attenuated the increase of BCRP and MDR1 expression induced by the miR-26b-5p inhibitor (Fig. 5e). Together, these data demonstrated that miR-26b-5p/SRGN axis regulates the expression of BCRP and MDR1 in drug-resistant BC cells.

miR-26b-5p regulates drug-response in xenograft mouse model

To assess the role of miR-26b-5p in drug response *in vivo*, 12 male immunodeficient nude mice were randomly divided into two groups ($n = 6$ in each group): (1) miR-NC group (injected with MCF-7/DOX and transfected with mim-NC), (2) miR-26b-5p mimic group (injected with MCF-7/DOX cells and transfected with miR-26b-5p mimic). Mice were also injected intravenously with 10 mg/kg DOX every 7 days after tumor cell inoculation. The miR-26b-5p mimic significantly reduced tumor growth and tumor weight (Fig. 6a and b). The expression of cell proliferation marker Ki-67 was also largely attenuated by the miR-26b-5p mimic (Fig. 6c). The presence of miR-26b-5p mimic also significantly reduced the level of SRGN expression in the tumor samples (Fig. 6e and f). Collectively, these data imply that miR-26b-5p/SRGN axis regulates drug responsiveness of BC cells *in vivo*.

Discussion

SRGN is a glycoprotein involved in the export of intracellular components, which seems to contribute to BC chemoresistance [13]. In this study, we validated SRGN as an indicator of chemotherapy resistance in BC patients based on the followed evidence: (1) SRGN is significantly upregulated in drug-resistant BC cell lines; (2) high expression of SRGN was found in the tissues of BC patients with chemotherapy resistance; (3) high expression of SRGN was strongly linked with tumor size, TNM stage, lymph node metastasis, and chemotherapy sensitivity; (4) silencing SRGN suppresses the expression of MDR proteins such as BCRP and MFR1, whereas SRGN overexpression upregulates BCRP and MRR1. BCRP and MRP1 are crucial multidrug-resistant proteins that confer drug resistance against many anticancer drugs, including conventional chemotherapeutics and targeted therapeutic agents [19,20]. Our research highlighted that SRGN upregulation may promote BCRP and MFR1 expression to confer chemotherapy resistance in BC cells. Targeting SRGN may serve as a potential intervention to overcome chemoresistance in BC patients.

Noncoding RNAs, which regulate the transcription of target genes by interfering with the transcription or modulating mRNA stability, are shown to be involved in a variety of cellular processes and pathological conditions [21–23]. For example, noncoding RNA metastasis-associated lung adenocarcinoma transcript 1 has been discovered as a marker for lung cancer metastasis [21]. LncRNA Haunt was reported to regulate HOXA gene activation during embryonic stem cell differentiation [23]. Notably, the dysregulation of noncoding RNAs is implicated in tumorigenesis [22]. Our research identified miR-26b-5p as an upstream regulator of SRGN, which negatively regulates SRGN to modulate drug sensitivity as follows: (1) miR-26b-5p binds to the 3′-UTR region of SRGN; (2) the expression level of miR-26b-5p is relatively lower in chemoresistant cell lines and tissues; (3) miR-26b-5p overexpression inhibits luciferase activity of SRGN reporter in BC cells; (4) miR-26b-5p inhibitor remarkably promotes SRGN expression, whereas miR-26b-5p overexpression significantly impairs the expression of SRGN.

miR-26b-5p also modulates the malignant phenotype of BC cells. miR-26b-5p mimic suppresses cell proliferation, migration, and invasion, whereas miR-26b-5p inhibitor shows opposite effects. Our data also demonstrated that miR-26b-5p/SRGN axis regulates the expression of BCRP and MDR1 in drug-resistant BC cells. Collectively, these results suggest that miR-26b-5p regulates chemosensitivity via SRGN-BCRP/MDR1 axis.

In conclusion, our data reveal the elevation of SRGN level and the downregulation of miR-26b-5p in drug-resistant BC cell lines and tissues. Moreover, we demonstrated that miR-26b-5p regulates chemoresistance in BC via SRGN-BCRP/MDR1 axis, which suggests that miR-26b-5p/SRGN axis may act as a novel target for BC treatment.

Acknowledgements

R.G.L. conceived and designed the experiments; Q.W.D. and X.L.H. performed the experiments and wrote the paper; Y.Q.H. and J.Z. analyzed the data. All authors approved the final version. All authors approved the final manuscript as submitted and agreed to be accountable for all aspects of the work.

The datasets used and/or analyzed during the current study are available from the corresponding author on reasonable request.

All procedures performed in studies involving human participants were in accordance with the ethical standards of the institutional and/or national research committee and with the 1964 Helsinki declaration and its later amendments or comparable ethical standards.

Informed consent was obtained from all individual participants included in the study.

Conflicts of interest

There are no conflicts of interest.

References

1 Harbeck N, Penault-Llorca F, Cortes J, Gnant M, Houssami N, Poortmans P, *et al*. Breast cancer. *Nat Rev Dis Primers* 2019; **5**:66.

2 Ji X, Lu Y, Tian H, Meng X, Wei M, Cho WC. Chemoresistance mechanisms of breast cancer and their countermeasures. *Biomed Pharmacother* 2019; **114**:108800.
3 Chuthapisith S, Eremin J, El-Sheemey M, Eremin O. Breast cancer chemoresistance: emerging importance of cancer stem cells. *Surg Oncol* 2010; **19**:27-32.
4 Samuel SM, Varghese E, Koklesová L, Líšková A, Kubatka P, Büsselberg D. Counteracting chemoresistance with Metformin in breast cancers: targeting cancer stem cells. *Cancers (Basel)* 2020; **12**:E2482.
5 Kartal-Yandim M, Adan-Gokbulut A, Baran Y. Molecular mechanisms of drug resistance and its reversal in cancer. *Crit Rev Biotechnol* 2016; **36**:716–726.
6 Gonzalez-Angulo AM, Morales-Vasquez F, Hortobagyi GN. Overview of resistance to systemic therapy in patients with breast cancer. *Adv Exp Med Biol* 2007; **608**:1–22.
7 Yousefi H, Maheronnaghsh M, Molaei F, Mashouri L, Reza Aref A, Momeny M, Alahari SK. Long noncoding RNAs and exosomal lncRNAs: classification, and mechanisms in breast cancer metastasis and drug resistance. *Oncogene* 2020; **39**:953–974.
8 Rinn JL, Chang HY. Genome regulation by long noncoding RNAs. *Annu Rev Biochem* 2012; **81**:145–166.
9 Vance KW, Ponting CP. Transcriptional regulatory functions of nuclear long noncoding RNAs. *Trends Genet* 2014; **30**:348–355.
10 Guo JY, Hsu HS, Tyan SW, Li FY, Shew JY, Lee WH, Chen JY. Serglycin in tumor microenvironment promotes non-small cell lung cancer aggressiveness in a CD44-dependent manner. *Oncogene* 2017; **36**:2457–2471.
11 Guo J-Y, Hsu H-S, Tyan S-W, Li F-Y, Shew J-Y, Lee W-H, Chen J-W. Serglycin in tumor microenvironment promotes non-small cell lung cancer aggressiveness in a CD44-dependent manner. *Oncogene* 2017; **36**:2457–2471.
12 Kori M, Gov E, Arga KY. Molecular signatures of ovarian diseases: insights from network medicine perspective. *Syst Biol Reprod Med* 2016; **62**:266-282.
13 Zhang Z, Qiu N, Yin J, Zhang J, Liu H, Guo W, *et al*. SRGN crosstalks with YAP to maintain chemoresistance and stemness in breast cancer cells by modulating HDAC2 expression. *Theranostics* 2020; **10**:4290-4307.
14 Xiang S, Dauchy RT, Hauch A, Mao L, Yuan L, Wren MA, *et al*. Doxorubicin resistance in breast cancer is driven by light at night-induced disruption of the circadian melatonin signal. *J Pineal Res* 2015; **59**:60–69.
15 Hoque MT, Shah A, More V, Miller DS, Bendayan R. *In vivo* and ex vivo regulation of breast cancer resistant protein (Bcrp) by peroxisome proliferator-activated receptor alpha (Pparα) at the blood-brain barrier. *J Neurochem* 2015; **135**:1113–1122.
16 Li S, Xu J, Yao Z, Hu L, Qin Z, Gao H, *et al*. The roles of breast cancer resistance protein (BCRP/ABCG2) and multidrug resistance-associated proteins (MRPs/ABCCs) in the excretion of cycloicaritin-3-O-glucoronide in UGT1A1-overexpressing HeLa cells. *Chem Biol Interact* 2018; **296**:45–56.
17 Taheri M, Mahjoubi F, Omranipour R. Effect of MDR1 polymorphism on multidrug resistance expression in breast cancer patients. *Genet Mol Res* 2010; **9**:34–40.
18 Trock BJ, Leonessa F, Clarke R. Multidrug resistance in breast cancer: a meta-analysis of MDR1/gp170 expression and its possible functional significance. *J Natl Cancer Inst* 1997; **89**:917–931.
19 Doyle L, Ross DD. Multidrug resistance mediated by the breast cancer resistance protein BCRP (ABCG2). *Oncogene* 2003; **22**:7340–7358.
20 Zyad A, Bénard J, Tursz T, Clarke R, Chouaib S. Resistance to TNF-alpha and adriamycin in the human breast cancer MCF-7 cell line: relationship to MDR1, MnSOD, and TNF gene expression. *Cancer Res* 1994; **54**:825–831.
21 Eissmann M, Gutschner T, Hämmerle M, Günther S, Caudron-Herger M, Gross M, *et al*. Loss of the abundant nuclear non-coding RNA MALAT1 is compatible with life and development. *RNA Biol* 2012; **9**:76–87.
22 Li L, Feng T, Lian Y, Zhang G, Garen A, Song X. Role of human noncoding RNAs in the control of tumorigenesis. *Proc Natl Acad Sci USA* 2009; **106**:12956–12961.
23 Yin Y, Yan P, Lu J, Song G, Zhu Y, Li Z, *et al*. Opposing roles for the lncRNA haunt and its genomic locus in regulating HOXA gene activation during embryonic stem cell differentiation. *Cell Stem Cell* 2015; **16**:504–516.